Rapid sex-specific evolution of age at maturity is shaped by genetic architecture in Atlantic salmon

Authors: Czorlich, Y.[1, 2], Aykanat T.[3], Erkinaro, J.[2], Orell P.[2] & Primmer, CR.[3, 4, 5*]

Affiliations**:**

[1] University of Turku, Department of Biology, Itäinen Pitkäkatu 4, FI-20520 Turku, Finland

[2] Natural Resources Institute Finland (Luke), POB 413, FI-90014 Oulu, Finland

[3] University of Helsinki, Organismal & Evolutionary Biology Research Programme, POB 56, FI-00014 Helsinki, Finland

[4] Institute of Biotechnology, POB 56, FI-00014 Helsinki, Finland

[5] Helsinki Institute of Sustainability Science, Faculty of Biological & Environmental Sciences, POB 56, FI-00014 Helsinki, Finland

[*]Corresponding author: craig.primmer@helsinki.fi

Abstract

Understanding the mechanisms by which populations adapt to their environments is a fundamental aim in biology. However, it remains challenging to identify the genetic basis of traits, provide evidence of genetic changes and quantify phenotypic responses. Age at maturity in Atlantic salmon represents an ideal trait to study contemporary adaptive evolution as it has been associated with a single locus in the *vgll3* region, and has also strongly changed in recent decades. Here, we provide an empirical example of contemporary adaptive evolution of a large effect locus driving contrasting sex-specific evolutionary responses at the phenotypic level. We identified an 18% decrease in the *vgll3* allele associated with late maturity (*L*) in a large and diverse salmon population over 36 years, induced by sex-specific selection during the sea migration. Those genetic changes resulted in a significant evolutionary response in males only, due to sex-specific dominance patterns and *vgll3* allelic effects. The *vgll3* allelic and dominance effects differed greatly in a second population and were likely to generate different selection and evolutionary patterns. Our study highlights the importance of knowledge of genetic architecture to better understand fitness trait evolution and phenotypic diversity. It also emphasizes the potential role of adaptive evolution in the trend toward earlier maturation observed in numerous Atlantic salmon populations worldwide.

Introduction

Understanding the mechanisms by which populations adapt to their environments is a fundamental aim in biology [1,2]. Such mechanisms may represent the only way for certain populations to persist in the face of strong human pressures and accelerated rates of climate change altering their environment. Temporal monitoring has documented recent and rapid phenotypic changes in wild populations in many species [e.g. 3,4]. However, whether or not such

45 phenotypic changes are adaptive often remains unclear [5,6]. Obtaining evidence of adaptive
46 evolution requires knowledge of the genetic basis of traits and subsequent demonstration that
47 natural selection induces changes in this genetic component [6]. Although the ideal strategy for
48 demonstrating adaptive evolution is to study the genes directly controlling the traits under
49 selection, such examples are extremely scarce [6,7]. Despite the increased availability of
50 genomic data, the identification of large-effect loci controlling phenotypes of ecological
51 significance and understanding how contemporary selection affects the allele frequency of
52 such genes remains indeed challenging [8]. In cases where the genetic architecture of a trait is
53 well characterized e.g. when a large-effect locus has been identified, retrospective genetic
54 analyses of archived material for the gene(s) controlling the trait in question can be
55 performed and provide detailed information about its evolutionary dynamics [e.g. 9].

56 Age at maturity in Atlantic salmon, defined here as the number of years spent at sea prior to
57 maturation, has recently been shown to be associated with a single large-effect locus with
58 sex-specific effects, located within a narrow (<100kb) region around the *vgll3* gene [10]. The
59 same locus has also recently been linked with gender-biased auto-immune diseases in humans
60 [11]. In Atlantic salmon, age at maturity reflects a classic evolutionary trade-off, as larger, later-
61 maturing individuals typically have higher reproductive success, but run a greater risk of
62 mortality before first reproduction. Sex-specific selection optima may exist for this trait [10].
63 Males generally mature earlier and at smaller size, whereas females mature later and have a
64 stronger correlation between body size and reproductive success compared with males [12]. It
65 was suggested that the sex-dependent dominance observed at *vgll3* partially resolves this
66 sexual conflict [10,13]. Furthermore, the age structure of many salmon populations has changed
67 worldwide in recent decades, generally towards an increasing proportion of smaller, earlier
68 maturing individuals [e.g. 14,15 but see 16]. However, the reasons for this, and whether it is an
69 adaptive change, remain unknown [17]. Therefore, age at maturity in Atlantic salmon provides a

rare opportunity to investigate the contemporary change of a phenotypic trait directly at the genetic level.

We studied a 40 year time series of two closely related Atlantic salmon populations from northern Europe with contrasting maturation age structure. Despite a low level of genetic divergence between them (F_{ST} = 0.012)[18], one population (Tenojoki) displays a high level of life-history diversity including a high proportion of large, later maturing individuals in both sexes, whereas the other population (Inarijoki) consists primarily of individuals of younger maturation ages, and with less life-history variation, particularly in males [15]. Here, we utilized a 40 year time series to detect potential signs of adaptive evolution in age at maturity by contrasting allele frequency changes at the maturation-linked gene *vgll3* with life-history phenotypes in 2500 samples from the two populations. We also investigated the occurrence of sex- and population-specific genetic architecture and selection, potentially explaining the observed diversity variation in age at maturity.

Results:

Temporal changes in age at maturity

We first quantified temporal phenotypic changes in both populations. There was a non-linear decrease in the age at maturity of Tenojoki individuals, with the mean maturation age of males declining by >40% (from 2.2 to 1.3 years; *edf* = 3.87, *F* = 5.11, P < 0.001) and of females by 8.1% (from 3.0 to 2.7 years; *edf* = 1.27, *F* = 0.57, P = 0.02), during the 36 year time period (Figure 1**a**). In Tenojoki males, the decrease occurred primarily between 1971 and 1987 before stabilization, while in females, age at maturity gradually decreased over the 36 year study period, explained best by a slightly nonlinear slope (Figure 1**a**). In comparison, Inarijoki males were virtually devoid of variation in age at maturity, with almost all males having spent one year at sea before maturing (*edf* = 0.00, *F*=0.00, P = 0.731), whereas mean

94 age at maturity in females fluctuated cyclically over the 37 years (*edf* = 10.14, *F* = 6.035, P <
95 0.001, Figure 1**b**), but with no indication of a decrease in average maturation age (Figure 1**b**).

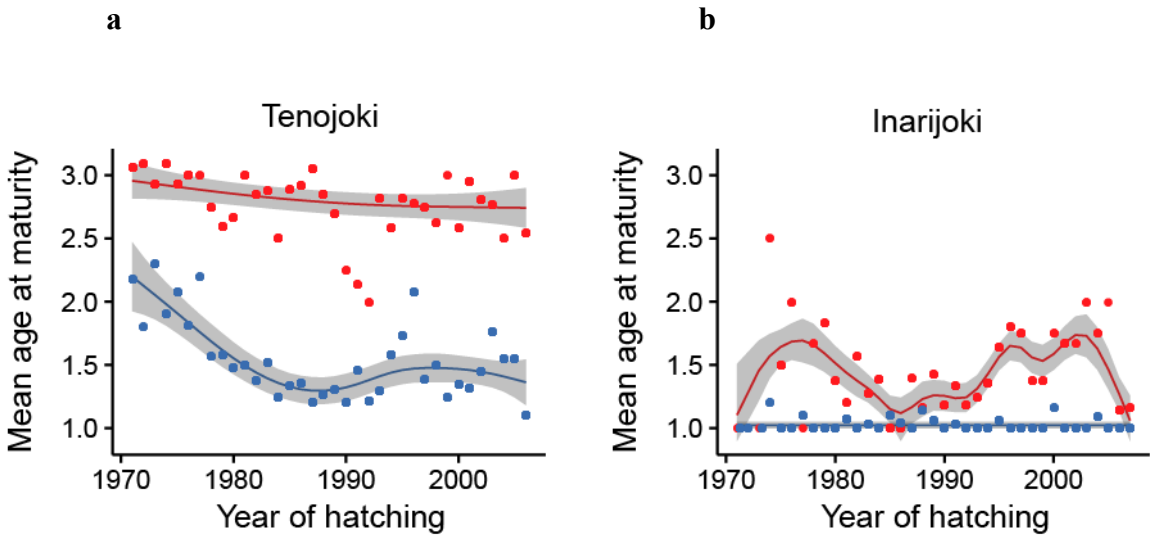

Figure 1: Change in mean age at maturity in the a, Tenojoki and b, Inarijoki populations.
Females are in red (*N* Tenojoki = 467, *N* Inarijoki = 261) and males in blue (*N* Tenojoki = 699, *N* Inarijoki = 570). Lines represent fitted values from the GAM ± 1.96 SE, points are observed annual means.

96 **Genetic architecture of age at maturity**

97 We hereafter use genetic architecture to refer to the additive and dominance effects of *vgll3*
98 on age at maturity. The *vgll3* genotypes had a sex-specific effect on the probability to observe
99 the different ages at maturity in the Tenojoki population ($\chi^2_{(6)} = 27.58$, P < 0.001). A sex-
100 specific dominance pattern was observed in this population; heterozygote males had a mean
101 age at maturity closer to homozygote *EE* (estimated dominance $\delta_M = 0.09$, $CI_{95} = [0.02,$
102 0.17], see Method) whereas heterozygote females had a phenotype closer to homozygotes *LL*
103 (estimated dominance $\delta_F = 0.80$, $CI_{95} = [0.65, 0.92]$; Figure 2**a**). In the Inarijoki population,
104 the *vgll3* genotypes were significantly associated with the probability to observe the different

105 age at maturity groups ($\chi^2_{(4)}$ = 56.41, P <0.001) but not in a sex-specific manner ($\chi^2_{(4)}$ = 8.27,
106 P = 0.08; estimated dominances of 0.13, CI_{95} = [0.05, 0.31] and 0.32 , CI_{95} = [0.17, 0.50] in
107 Inarijoki males and females, respectively). Differences in mean age at maturity between
108 homozygotes varied depending on the sex and population (i.e. additive or allelic effect: effect
109 of the substitution of one allele for the other). In the Tenojoki population, the relative
110 difference in mean age at maturity between alternative *vgll3* homozygotes was about three
111 times higher in males (+106% for *LL*, +1.17 years, CI_{95} = [0.99, 1.33]) than in females (+32%
112 for *LL*, +0.71 years, CI_{95} = [0.51, 0.91]). This pattern was inverted in Inarijoki, with the
113 relative difference in mean age at maturity between female homozygotes being about six
114 times larger (+74% for *LL*, +0.94 years, CI_{95} = [0.68, 1.25]) than in males (+12% for *LL*,
115 +0.13 years, CI_{95} = [0.05, 0.22], Figure 2**b**). These results imply that selection during the sea
116 migration, defined as the relative difference in survival between genotypes, is likely to vary
117 between sexes and populations. There was no statistically significant change in the effect size
118 of *vgll3* on maturation age over time in either population (Tenojoki: $\chi^2_{(6)}$ = 6.07, P = 0.42;
119 Inarijoki: $\chi^2_{(4)}$ = 4.41, P = 0.35).

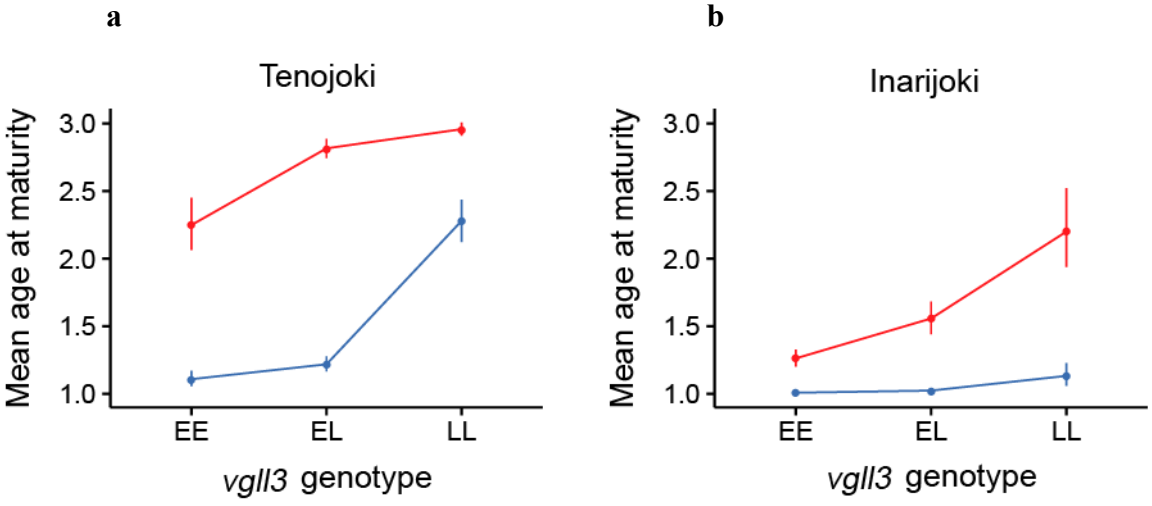

Figure 2: Mean age at maturity as a function of *vgll3* genotype in the a, Tenojoki and b, Inarijoki populations.
Females are in red (*N* Tenojoki = 522, *N* Inarijoki = 286) and males in blue (*N* Tenojoki = 804, *N* Inarijoki = 612). Means are calculated from multinomial models fitted values, averaged over years. Error bars represents 95% bootstrap confidence intervals based on 1000 replicates.

120 **Evolution of *vgll3* and signals of selection**

121 The *vgll3* late maturing (*L*) allele frequency decreased significantly, from 0.66 to 0.54 (18%)
122 in 36 years, in the Tenojoki population ($F_{(1)}$ = 7.80, P = 0.009; log-odd slope = -0.014 (CI_{95} =
123 [-0.004, -0.024]; Figure 3**a**). This allele frequency change was the highest of all the 144
124 genome-wide SNPs assessed and could not be explained by drift alone ($P_{\Delta_{vgll3}}$ = 0.004,
125 Figure 3**a**), nor after accounting for sampling variance ($P_{\Delta_{vgll3}}$ = 0.022). This observation
126 provides strong support for natural selection acting against the *vgll3 L* allele in the Tenojoki
127 population (see supplementary material). In the Inarijoki population, the trend in the *vgll3 L*
128 allele frequency was also negative (log-odd slope ≈ -0.009, CI_{95} = [-0.023, 0.006] but not
129 significant ($F_{(1)}$ = 1.29, P = 0.26, Figure 3**b**). About 10% of the 134 genome-wide SNPs
130 assessed had a larger change in allele frequency than *vgll3* in this population (Figure 3**b**).
131 Consequently, we could not rule out drift as the basis of this change ($P_{\Delta_{vgll3}}$ = 0.189 for drift,
132 and $P_{\Delta_{vgll3}}$ = 0.292 after accounting for sampling variance).

133 To further quantify the strength of selection driving changes in *vgll3* allele frequency, a
134 Bayesian model was used to estimate selection coefficients whilst accounting for genetic
135 drift, similar to a Wright-Fisher model (see Methods). The selection coefficient in the
136 Tenojoki population was large and significantly higher than zero, albeit with large credibility
137 intervals (-*s* = 0.33 (95% credibility interval = [0.01, 0.77], Supplementary Figure 1). In
138 Inarijoki, there was no evidence for significant selection (*s* = 0.25, CI_{95} = [-0.08, 0.49]).

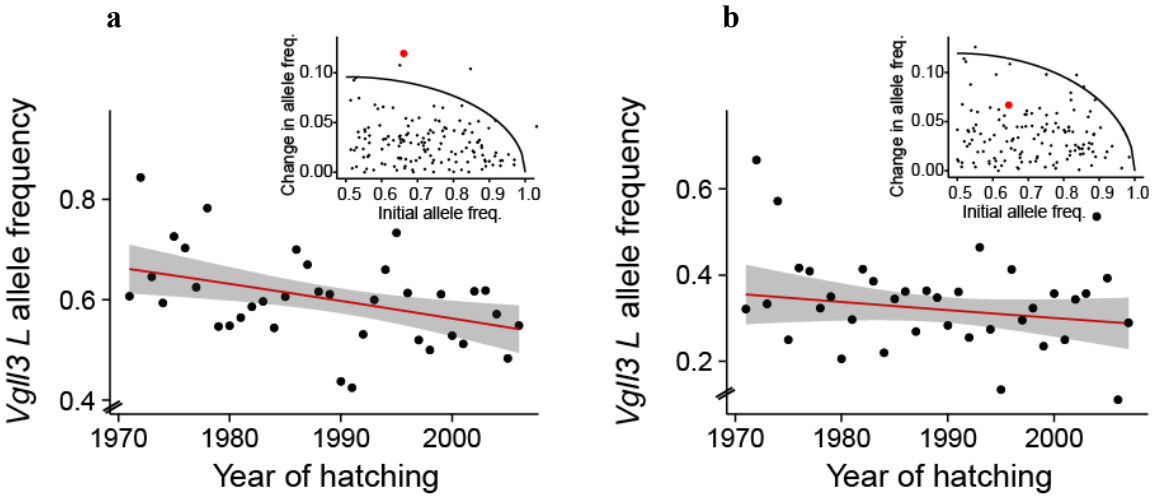

Figure 3: Temporal changes in *vgll3 L* allele frequency associated with late maturation in the a, Tenojoki and b, Inarijoki populations.
The lines represent fitted values from the quasibinomial model with ± 1.96 SE (*N* Tenojoki = 1166, *N* Inarijoki = 765). The *vgll3* log-odd slope was estimated at -0.014 (CI95 = [-0.004, -0.024], P = 0.009) in Tenojoki and -0.009 (CI95 = [-0.023, 0.006], P = 0.26) in Inarijoki. Insets show the absolute estimated changes in allele frequencies of each SNP as a function of initial allele frequency in **a**, Tenojoki (144 loci) and **b,** Inarijoki (135 loci) over 36 and 37 years, respectively. The line represents the expected amount of drift at the 97.5 quantile. The *vgll3* locus is indicated in red.

The *vgll3 L* allele frequency differed between sexes in a contrasting manner in the two populations. The odds of possessing an *L* allele was 37% higher in females than in males in the Tenojoki population (CI_{95} = [0.12, 0.69], $F_{(1)} = 8.72$, P < 0.01, Figure 4) but 53% lower in Inarijoki (CI_{95} = [0.40, 0.65], $F_{(1)} = 36.51$, P < 0.001, Figure 4). This could be the result of either sex- and genotype-specific fertilization ratio or juvenile mortality in freshwater, or alternatively, selection at the *vgll3* locus differing between the sexes during sea migration, prior to returning to reproduce. In order to distinguish the latter possibility (selection at sea) from options involving selection during the freshwater phase we genotyped 143 and 108 juveniles of various ages collected from the same freshwater locations in Tenojoki and Inarijoki (1-3 years old, see Methods), respectively. Juvenile sex ratios were close to parity and the *vgll3 L* allele frequency was similar in both sexes in both populations ($\chi^2_{(1)} = 3.27$, P = 0.07 in Tenojoki, $\chi^2_{(1)} = 0.04$, P = 0.85 in Inarijoki, Figure 4). This provides support for the notion that selection strength acting on the *L* allele varies in a sex-specific manner during the

152 marine life-history phase, as opposed to during the freshwater juvenile phase. Such sex-
153 specific allele frequency patterns may be reinforced by sex-specific dominance
154 (Supplementary Figure 2).

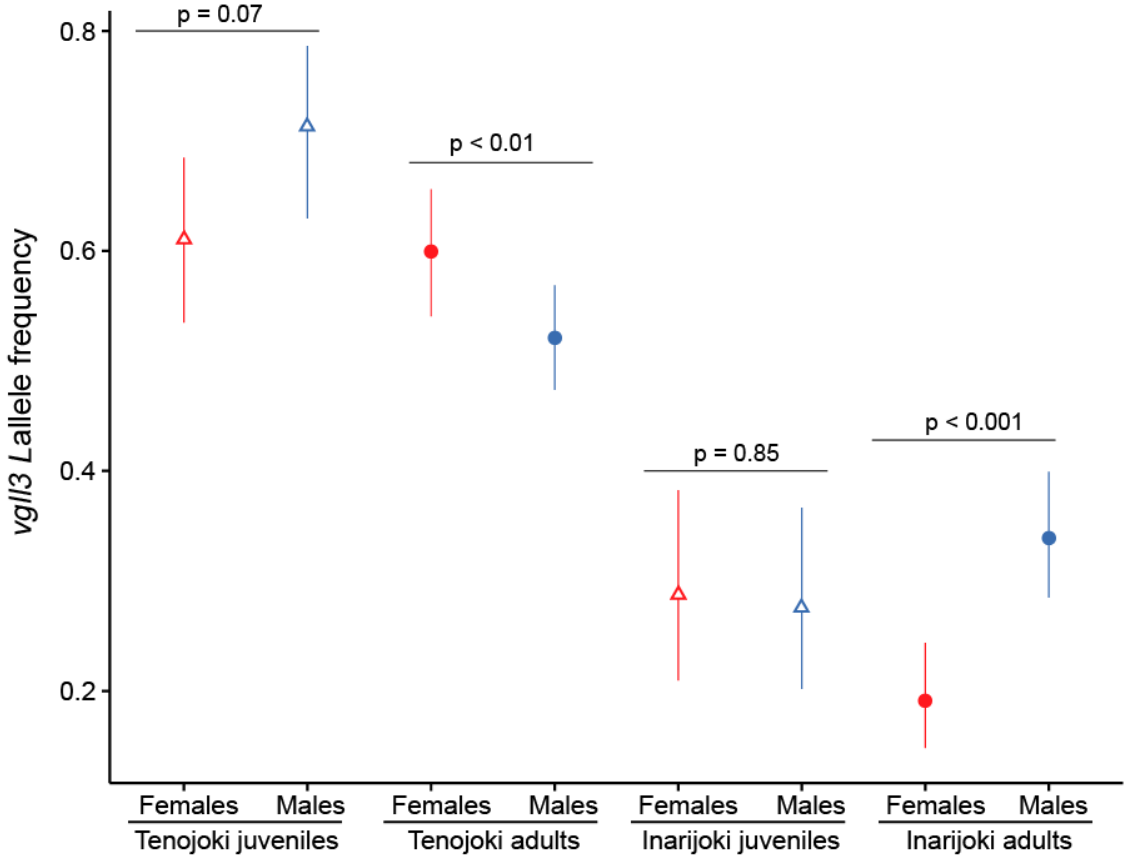

Figure 4: Model predicted mean *vgll3 L* allele frequency as a function of the sex and reproductive status in Tenojoki and Inarijoki.
Error bars indicate 95% confidence intervals. Adult allele frequencies are from years 2006 and 2007 for females (red circles) and males (blue circles), respectively, in the Tenojoki and Inarijoki populations. Juveniles allele frequencies (triangles) are from 2012 in Tenojoki (2-3 years old) and 2016 in Inarijoki (1-3 years old).

155 **Sex-specific evolutionary response**

156 In Tenojoki, the sex-specific genetic architecture drove contrasting evolutionary responses in
157 the two sexes. Temporal changes in genotypes explained about 50% of the non-linear
158 decrease in male age at maturity (0.46 years, $edf = 3.95$, $F = 3.51$, $P < 0.001$; Supplementary

Figure 3) but didn't explain the temporal changes in female age at maturity (0 years, *edf* = 0, $F = 0.00$, P = 0.54). Temporal changes in genotype frequencies were similar between sexes ($\chi^2_{(2)} = 2.78$, P = 0.25) and were thus unlikely to be the main driver of those sex-specific evolutionary responses. On the other hand, both the dominance patterns and *vgll3* effect sizes varied greatly between sexes (Figure 2**a**) and could contribute to the different responses. For instance, an individual with the *EE* genotype rather than *LL* matures, on average, 0.71 (CI_{95} = [0.51, 0.91]) or 1.17 (CI_{95} = [0.99, 1.33]) years earlier, depending whether it is a female or a male. The extent of the phenotypic response thus differs between the sexes for a similar *EE* genotype frequency change. Further, because of sex-specific dominance, the phenotypic response to a change in heterozygote frequency will also vary between the sexes. For example in Tenojoki females, the phenotypic change induced by a decrease in the *LL* genotype frequency would be partially compensated by the increase in the *EL* genotype frequency, which results in a similar phenotype distribution due to the dominance of the *L* allele (Figure 2**a**, Supplementary Figure 4). In contrast, in males, the recessivity of the *vgll3 L* allele ($\delta_M = 0.09$) would favor a larger decrease in age at maturity when the proportion of *EL* heterozygotes is increasing. Most of the observed decline in female age at maturity could be explained by the spawning year (0.20 year, *edf* = 2.16, F=21.61, P < 0.001). The year effect also explained a part of the decline in male age at maturity (0.15 year, *edf* = 2.126, F = 12.41, P < 0.001).

Discussion

We provide convincing evidence of rapid adaptive evolution of age at maturity toward small, early-maturing individuals in a large Atlantic salmon population. This indicates that despite having a reproductive advantage due to their large size [12,19], the late maturation life-history strategy has become increasingly costly and modified the reproductive success vs survival

183 trade-off such that earlier maturation is increasingly advantageous. Adaptive evolution may
184 thus represent a realistic mechanism behind changes towards earlier age at maturity observed
185 worldwide in the last decades in Atlantic salmon [e.g. 14–16,20] and other salmonid fish species [e.g.
186 21]. What could be the causes of such rapid evolution of a life-history trait? One explanation is
187 that it could be linked to recent rapid changes in the marine environment of the Teno salmon
188 populations. For example, climate change may negatively affect Atlantic salmon marine
189 growth and/or survival directly [e.g. 22] or indirectly through changes in Arctic food-webs and
190 ecosystem functioning resulting from e.g. species range expansions [20,23,24]. Atlantic salmon
191 occupying the northernmost parts of the globe will be unable to move to a colder climate in
192 response to ocean warning, which would reinforce the importance of adaptation for
193 population persistence. Another possibility is human-induced evolution of age at maturity
194 through fishing targeting Atlantic salmon differentially according to their size, and therefore
195 age at maturity [e.g. 25,but see 26], or reducing prey abundance [e.g. 27]. Such environmental changes
196 and/or human-induced pressure could negatively affect salmon survival at sea and thus
197 increase the cost of late maturation, thereby potentially tipping the selective balance such that
198 the size advantage at reproduction stemming from spending additional years at sea no longer
199 compensates for the increased mortality and thus drives evolution towards younger
200 maturation age. It is important to note however, that natural selection didn't entirely explain
201 the observed temporal changes in age at maturity in the Tenojoki population. Irrespective of
202 the *vgll3* genotypes, the probability to mature at younger ages, after one or two years at sea,
203 increased over time (Supplementary Information). This could be due to adaptive phenotypic
204 plasticity [28], through changes in maturation probability towards the same direction as
205 selection, or to changes in allele frequencies of, as yet unknown, smaller effect loci. Further
206 investigation is required to test these hypotheses. Regardless, such changes in population age
207 structure can negatively affect the population growth rate and/or temporal stability induced

via portfolio effects [e.g. 29] and also have negative consequences on genetic diversity levels [e.g. 30] and thus are a concern for future population persistence.

Despite common temporal changes in *vgll3* allele frequency between the sexes, differing genetic architectures, in terms of additive and dominance patterns, contributed to sex-specific selection strengths and evolutionary responses to selection. We observed sex-specific differences in *vgll3* allele frequencies in adult salmon that were not present in pre-marine-migration juveniles from the same populations (Figure 4). Interestingly, the direction of the sex-specific differences was opposite in the two populations studied. The combined effects of sex-dependent dominance and sex-specific selection patterns can explain these contrasting patterns. Indeed, large between-populations variation in *vgll3* effects on age at maturity may influence selection and adaptive responses of individuals. The relative strength of allelic effects differed dramatically between sexes and these effects were in opposite directions in the two populations: in Inarijoki, the difference in mean age at maturity between homozygotes is about six times larger in females compared to males whereas in Tenojoki, the relative difference was three times higher in males (Figure 2). Therefore, selection against *LL* genotype individuals acts primarily on females in Inarijoki, but on males in Tenojoki (Figure 4, Supplementary material). However, sex-specific dominance also plays a role by introducing differences in allele frequencies between sexes that are dependent on population allele frequency (Supplementary Figure 2). Furthermore, sex-specific genetic architectures induce sex-specific evolutionary responses in Tenojoki, by accelerating the decrease in age at maturity in males and reducing the temporal phenotypic variation in females. Sex-specific dominance is likely to have evolved to reduce intra-locus sexual conflict [10]. However, whether this genetic architecture is presently at its optimum is questionable in light of the quick decrease in *vgll3 L* allele frequency and age at maturity. Further studies are necessary to determine whether sexually antagonistic selection in Tenojoki is persisting in ever

changing environments and to describe the extent, origin and consequences of among population variation in genetic architecture.

Age at maturity evolved rapidly under sex-specific selection in just 36 years, equivalent to 4-6 generations in Atlantic salmon. Despite being genetically similar, the two studied populations had distinctive genetic architectures, sex-specific selection and consequently *vgll3* allele frequencies variation. This study shows that variability in genetic architectures can create complex selection and evolutionary patterns between sexes and populations. This highlights the importance of determining the genetic basis of fitness traits in order to better understand their evolution and to explain the phenotypic diversity observed between populations and species.

Material and methods

Study site and sampling

The subartic Teno River forms the border between Finland and Norway and drains north into the Barents sea (68 - 70ºN, 25-27ºE). Genetically distinct salmon populations [31] are distributed throughout the 16 386 km^2 catchment area. Annual river catches range from about 20,000 to 60,000 individuals, representing up to 20% of the entire riverine Atlantic salmon harvest in Europe [32]. Atlantic salmon populations from Teno have been monitored since early 1970s with collections of scales and phenotypic information by trained fishers[15,33]. Scales were stored in envelopes at room temperature and used to determine individual life-history characteristics including the number of years spent in the freshwater environment prior to smoltification (river age), number of years spent in the marine environment prior to maturation (sea age) and possible previous spawning events, following international guidelines (ICES 2011). The Teno river Atlantic salmon have diverse life history strategies [15,35]. They can spend from two to eight years in freshwater before smoltifying, from one to

five years at sea before maturing and have up to five breeding attempts. Overall, a total of 120 combinations of river age, sea age at maturity and repeat spawning strategies have been described [15]. Age at maturity has been declining in Teno salmon over the last 40 years, with proportionally fewer late maturing salmon returning over years. Age at maturity also differs largely among populations displaying genomic signatures of local adaptation [15,33].

We randomly selected scales from individuals caught by rod between 1972 and 2014 during the later part of the fishing season, from July 20 to August 31. Most of the Teno salmon are expected to have reached their home river by late July [36]. Samples came from two different locations, the middle reaches of the Tenojoki mainstem (hereafter Tenojoki) and a headwater region Inarijoki (Supplementary Figure 5). These sections of the river host weakly differentiated salmon populations with contrasting sea-age structure at maturity [31,33]. Individuals from the Tenojoki spend, on average, more time at sea before maturing than individuals from the Inarijoki population [15,30]. Seventy additional females were selected in Inarijoki over the study period, by following the same sampling scheme, to increase the sampling size in analyses with sex-specific estimates. Scale or fin samples were also collected from juvenile salmon from the Tenojoki (N=143, 2-3 years old) and Inarijoki (N=108, 1-3 years old) populations caught by electrofishing in the 2012 and 2016, respectively. They were used as the baseline for population assignment of adults and to determine potential sex-specific *vgll3* allele frequency differences at the juvenile stage.

Genotyping

DNA extraction from scales, sex determination and genotyping were performed following [37]. In total, 2482 individuals were genotyped at 191 SNPs, including the SNP the most highly associated with the age at maturity, *vgll3TOP* (vestigial-like family member 3 gene also called *vgll3,* [10]) and outlier and baseline SNP modules [37]. The outlier module consisted of 53

SNPs highly differentiated between the Inarijoki and Tenojoki populations, thus allowing a more powerful assignment of population of origin, between these two closely related populations [i.e. see 30,37].The baseline module included 136 putatively neutral markers in low linkage disequilibrium, distributed over the whole genome proportionally to chromosome length, previously filtered to have minor allele frequency >0.05 and heterozygosity >0.2[37]. These SNPs were used to estimate the level of differentiation among populations of the Teno River (Weir and Cockerham's F_{ST}) and genetic drift. Mean genotyping success was on average 0.80 per locus and individual.

Population assignment

The 53 outlier loci were used to determine the optimum number of genetic clusters and assign the population of origin of adults using the software STRUCTURE. First, an admixture model with correlated allele frequencies [38] was run on adult and juvenile data for 80,000 MCMC iterations, including a burn-in length of 50,000. The model was replicated six times for each cluster value K, varying from one to four. The optimal number of clusters was thereafter estimated using the Δ K method described in Evanno, Regnaut, and Goudet (2005) using STRUCTURE HARVESTER [40]. This allowed us to determine whether juveniles were correctly assigned to their sampling locations and could thus be used as a baseline for adult assignment. Then another admixture model with correlated allele frequencies was replicated six times on adult data using juvenile data as a baseline, with prior migration set to 0. The *fullsearch* algorithm from the CLUMP software (Jakobsson & Rosenberg 2007) was used to account for across replicate variability in membership coefficients. Finally, the cluster of each adult was assigned by using the optimum K and membership probability superior or equal to 0.8. The differentiation between populations was tested by calculating the likelihood ratio G-

304 statistic [41] and comparing it with the G-statistic distribution obtained by permuting 1,000
305 times individuals between populations.

306 The most likely number of clusters determined with the Δ K method was two when juveniles
307 and adults data were combined (Supplementary Figure 6Supplementary Figure 6). Juveniles
308 were assigned accordingly to their sampling location in more than 96% of cases
309 (Supplementary Figure 7). Using juvenile data as a baseline, 90% of adults were classified to
310 one of the two clusters with probabilities equal or higher than 0.8. Individuals sampled in
311 Tenojoki were assigned to the Inarijoki population in 25% of the cases whereas only 2% of
312 the individuals caught in Inarijoki were assigned to the Tenojoki population. In total, 1330
313 and 911 individuals clustered in the Tenojoki and Inarijoki populations, respectively
314 (Supplementary Figure 8). The two populations were significantly genetically differentiated
315 (F_{ST} = 0.013, G = 201.55, P < 0.01) and had contrasted age structures (Supplementary Figure
316 9).

317 # Statistical analyses

318 ### Temporal variation in age at maturity and proportion of females

319 Non-linear temporal variation in age at maturity was estimated separately for each population
320 using generalized additive models, with the Gaussian family as the residual distribution. Year
321 of hatching was included as an independent variable inside a cubic regression spline for each
322 sex. The study included spawning individuals caught over a 43 year period (1972 to 2014).
323 Hatch years were calculated based on the specific life-history strategy of each individual and
324 spanned the period from 1971 to 2006 in Tenojoki and 1971 to 2007 in Inarijoki. Sex was
325 also included as an explanatory variable.

326 The amount of smoothing was determined in each case using the maximum likelihood
327 method. Automatic smoothness selection was performed by adding a shrinkage term. The
328 significance of independent variables was assessed using F-tests and an alpha risk of 0.05. All
329 statistical tests included in this manuscript were two-tailed. The additive models were run with
330 the R package *mgcv* [42,43].

331 **Effect size of *vgll3* on age at maturity**

332 To estimate the genetic effect of *vgll3*, age at maturity was also regressed using a multinomial
333 model separately for each population. In Tenojoki, two individuals having matured after five
334 years at sea were considered having matured after four years to avoid the estimate of
335 additional model parameters without data support. The sex, year of capture and *vgll3*
336 genotype can all influence age at maturity and were included in models as a three-way
337 interaction. Multinomial models in this study were performed using the R package nnet [44].
338 Model selection was performed using backward selection with F-tests and by calculating the
339 AICc of all possible models. The effect of year on the probability to mature was calculated
340 with the Effect package [45] which averages the effect size across sexes and genotypes. The
341 mean age at maturity per sex and genotype was calculated from model predicted values. First,
342 predicted age was obtained for each year, sex and age at maturity combination by multiplying
343 the probabilities of having matured after one, two, three or four years at sea by the
344 corresponding sea age at maturity and taking the sum. Second, the age at maturity was
345 calculated for each sex and genotype by averaging over years. This process was replicated
346 1000 times by randomly sampling with replacement and fitting a new model. A 95%
347 bootstrap confidence interval was then determined by taking values of the 2.5 and 97.5
348 percentiles. The *vgll3* alleles were called *L* and *E* to indicate their association with late and
349 early maturation, respectively [10]. Dominance for each sex and population was estimated from

the mean age at maturity (μ) following $\delta = \frac{\mu_{EL} - \mu_{EE}}{\mu_{LL} - \mu_{EE}}$. The *L* allele is recessive if $\delta = 0$, additive if $\delta = 0.5$ and dominant if $\delta = 1$.

To determine how much of the observed changes in age at maturity over time could be attributed to changes in genotypes and year of capture, a new dataset with the spawning year held constant at 1975 was created for Tenojoki. The previous multinomial model was used to predict new maturation probabilities from which model predicted age at maturity were calculated for each individual, as above. Temporal changes in age at maturity attributed to genotypes were determined by fitting a generalized additive model using the Gaussian family and including the individual hatch year in a cubic regression spline and the sex as independent variable. Changes in age at maturity attributed to the year of capture corresponded to the difference between individual predicted age at maturity calculated from the original dataset and the one with the year fixed. Another Gaussian generalized additive model was also performed on those differences, by including the hatch year in a cubic regression spline. Automatic smoothness selection was performed by adding a shrinkage term.

Change in allele and genotype frequencies

Temporal variation in allele frequencies was determined for each population and locus using generalized linear models (*glm*), with the quasibinomial family to account for overdispersion. Sex-dependent *vgll3* genetic effect on the age at maturity [10] may create sex-specific selection at sea, leading to differences in *vgll3* allele frequency between male and female spawners from the same generation. The sex variable can capture this potential intra-generation variation in allele frequency. Hence, sex and year of hatching were included as independent variables in the *glm*. To keep the potential effect of sex-specific selection on the *vgll3* allele

373 frequency temporal change, the model was also run without including sex as a covariate. The
374 significance of variables was assessed with F-tests.

375 In order to determine whether *vgll3* allele frequencies varied across time more than under the
376 neutral expectation, model predicted temporal changes in allele frequencies were compared
377 among loci with individual genotyping success higher than 0.7 (144 and 135 loci for the
378 Tenojoki and Inarijoki populations, respectively). This threshold was chosen as a trade-off
379 between increasing the quality and amount of data per locus (average genotyping success
380 superior to 0.90 in those subsets) and keeping a large number of loci for the comparison
381 (~25-30% of loci were excluded). The amount of genetic drift, and thus random temporal
382 allele frequency change, is dependent on the initial allele frequency of each locus [46]. The
383 comparison of temporal changes between *vgll3* and other putatively neutral loci was thus
384 corrected for initial allele frequency by calculating the expected amount of drift at *vgll3* under
385 a Wright-Fisher model [47,48]. The distribution of allele frequency $x(t)$ after t generations can
386 be approximated using a normal distribution [46]:

$$x(t)|x(0) \sim Normal\ (x(0), x(0)\big(1 - x(0)\big)\frac{t}{2N})$$

387 with $x(0)$ being the initial allele frequency and *N* the effective population size. The ratio
388 $\zeta = \frac{t}{2N}$ was estimated with a Bayesian model using a uniform prior distribution ranging from
389 0 to 1. The binomial fitted allele frequencies at birth for years 1971 ($x(0)$) and 2006 ($x(t)$) in
390 Tenojoki and 1971 ($x(0)$) and 2007 ($x(t)$) in Inarijoki were used as data for all loci except
391 *vgll3*. Two MCMC chains were run for 100,000 iterations with thinning interval 10, and a
392 burn-in length of 100,000. Convergence was assessed using the Gelman and Rubin's
393 convergence diagnostic[49] and a potential scale reduction factor (*psrf*) threshold of 1.1. The
394 probability to observe the *vgll3* allele frequency change ($\Delta_{vgll3} = |x(t)_{vgll3} - x(0)_{vgll3}|$)

395 under drift alone was calculated at each of the 20,000 saved iterations (i) to account for
396 uncertainty in ζ estimation as follows:

$$P_{\Delta_{vgll3}} = \frac{1}{20000} \sum_{i=1}^{20000} [\Delta_{drift\,i} \geq \Delta_{vgll3}]$$

397 with

$$\Delta_{drift\,i} = |x(t)_i|x(0)_{vgll3} - x(0)_{vgll3}|)$$

398 and

$$x(t)_i|x(0)_{vgll3} \sim Normal\,(x(0)_{vgll3}, x(0)_{vgll3}(1 - x(0)_{vgll3})\zeta_i)$$

399 To account further for uncertainty in *vgll3* allele frequency change, Δ_{vgll3} was re-estimated at
400 each iteration *i* by running the quasi-binomial model with a new dataset, sampled for each
401 year from the original dataset with replacement. The distribution of changes expected under
402 drift alone was also calculated in the same manner as for *vgll3*, for initial allele frequencies
403 $x(0)$ varying from 0.5 to 1.

404 To determine whether potential differences in *vgll3* allele frequencies between adult males
405 and females are likely to arise during the sea migration, juvenile allele frequencies were
406 analyzed using a separate *glm* with the binomial family for each population. Sex was
407 introduced as an independent variable. A backward model selection was performed using
408 Likelihood-Ratio Tests (LRT) and an alpha risk of 0.05. Confidence intervals were calculated
409 with the lsmean package [50] by taking the years 2006 and 2007 as reference for the Tenojoki
410 and Inarijoki adults, respectively.

411 To further describe temporal changes in *vgll3* genotypes, a multinomial model was used for
412 each population. The year of hatching and the sex were introduced as independent variables

in a two way interaction. A backward model selection was performed using LRT and an alpha risk of 0.05.

Allele frequencies may differ between sexes due to sex-specific selection between homozygotes but also because of the effect of sex-specific dominance, even when selection is sex-independent. To determine how dominance can contribute to differences in allele frequencies between sexes in the latter case, the expected sign and magnitude of allele frequency differences were determined for different selection strengths, by using the dominance patterns calculated previously for the Inarijoki and Tenojoki populations. Considering a gene with 2 alleles *A* and *B* with respective frequencies *p* and *q*, the allele frequency after a selection event corresponds to:

$$p_s = \frac{p^2 W_{AA} + pq\, W_{AB}}{p^2 W_{AA} + 2pq W_{AB} + q^2 W_{BB}}$$

with W_{AA}, W_{AB} and W_{BB} the relative fitness of each respective genotype:

$W_{AA} = 1;\ W_{AB} = 1 - DS$ and $W_{BB} = 1 - S$.

where S is the selection coefficient common to each sex, varying from 0 to 0.90 by 0.15 intervals. *D* is the dominance coefficient. P_s was calculated for each sex and population using the corresponding dominance coefficients previously calculated from phenotypes (δ) and an initial *p* varying from 0 to 1. The expected difference in allele frequency in Supplementary Figure 2 corresponds to p_s(female) - p_s(male), calculated for each combination of S and *p*.

Estimation of selection coefficients

A Bayesian model was used to estimate selection coefficients by accounting for drift induced by a limited number of spawners, in a similar way to Wright-Fisher models [e.g. 51,52].

First, the linkage disequilibrium method [53] implemented in the software NeEstimator 2.01 [54] was applied on samples grouped by cohort year to estimate the parental effective number of breeders (*N*b). This approach was favored over the standard temporal method potentially generating biased effective size estimates when used with temporally close samples from species with overlapping generations [55] and only providing information about the harmonic mean of effective sizes. In order to use the linkage disequilibrium *Nb* values and associated 95% parametric confidence intervals in the Bayesian models, parameters of log-normal distributions with similar percentiles were assessed using the R package *rriskDistributions* [56]. Weights of 7, 2 and 1 were respectively assigned to the 2.5, 5.0 and 97.5 percentiles to increase the approximation precision for lower bounds and medians. The negative or infinite values were replaced by 5000 or 10 000 for the median and 95% confidence interval upper bound, respectively. These are realistic maximum breeder numbers in the populations and represent a conservative approach. If the lower bound also displayed infinite values, the corresponding distribution had a median of 9 000 and lower and upper bounds of respectively 8 000 and 10 000.

The selection coefficient represents "the reduction in relative fitness, and therefore genetic contribution to future generations, of one genotype compared to another" [57]. Selection coefficients were estimated using 32 and 33 different spawning years, with corresponding hatch years, for Tenojoki and Inarijoki, respectively. Considering a SNP with alleles A1 and A2 and $W_y^{11} = 1$, $W_y^{12} = 1 - DS$ and $W_y^{22} = 1 - S$ being the relative fitness of each genotype. S corresponds to the selection coefficient, following a uniform prior distribution ranging from -1 to 1. D denotes the dominance coefficient, following a uniform prior distribution ranging from 0 to 1 . The observed number of each genotype g in spawners of sex s in year y ($O_{g,s,y}$) followed a Dirichlet Multinomial (DM) distribution:

$$O_{g,s,y} \sim DM(T_{s,y}, g_{s,y}^{11} \dots g_{s,y}^{22}, \eta)$$

where η is the variation parameter following a uniform distribution ranging from 1 to 2500 and $T_{s,y}$ the total number of spawners per sex and year. The spawners genotype frequency for each sex ($g_{s,y}^{11} \dots g_{s,y}^{22}$) varied over years according to a hierarchical model, $g_{s,y}^{11} \dots g_{s,y}^{22} \sim \text{dirichlet}\,(\mu g_s^{11} \dots \mu g_s^{22}\, \eta)$ and $\mu g_s^{11} \dots \mu g_s^{22} \sim \text{dirichlet}\,(1,1,1)$. The observed number of allele A1 (n_y) in individuals born in year y follow a binomial distribution:

$$n_y \sim Binomial(p_y, 2\, N_y)$$

with N_y being the total number of individuals per year and p_y the population allele frequency. The expected allele frequency in the cohort y depends on genotype frequency in spawners the year before as follows:

$$E[p_y] = \frac{g_{y-1}^{11} W^{11} + 0.5\, g_{y-1}^{12} W^{12}}{\bar{W}}$$

with $\bar{W}$ being the population mean fitness $\bar{W} = g_{y-1}^{11} W^{11} + g_{y-1}^{12} W^{12} + g_{y-1}^{22} W^{22}$. g_{y-1}^{11}, g_{y-1}^{12} and g_{y-1}^{22} are the genotypes of spawners averaged across sexes, as each sex contributes equally to the next generation despite a potential biased sex-ratio. Genetic drift should be taken into account to estimate p_y from the genotype frequencies of the previous year's spawners. In populations with random mating, it corresponds to drawing randomly p_y from a binomial distribution [46–48] with as parameters the expected allele frequency E[py] and twice the effective number of spawners, previously estimated with the linkage disequilibrium method ($2\, Nb_y$). Consequently, the expected variance of the allele frequency p_y subject to drift is after one generation $Var(p_y) = \frac{p_y(1-p_y)}{2\, Nb_y}$. For computing time and convergence reasons, a beta distribution with equal mean and variance was used instead:

$$p_y \sim Beta(\alpha, \beta)$$

with

$$\alpha = \frac{E[p_y](Var(p_y)+E[p_y]^2-E[p_y])}{Var(p_y)} \quad \text{and} \quad \beta = \frac{(Var(p_y)+E[p_y]^2-E[p_y])(E[p_y]-1)}{Var(p_y)}$$

Priors used in this model were chosen to be as uninformative as possible. For the *vgll3* locus, the *L* allele was chosen as reference. The "pMCMC" were calculated from the two chains as following: 2 * min(p < 0; 1 - p < 0), p<0 being the proportion of values below zero.

Posterior distributions were approximated using Monte Carlo Markov Chain (MCMC) methods with the Just Another Gibbs Sampler software (JAGS [58]) run in the R environment [43]. Two MCMC chains were run for 4.5 million iterations, including a burnin length of 3.5 million. Only one iteration out of 100 was kept to reduce the memory size used. Gelman and Rubin's convergence diagnostic [49] was used to assess convergence. Models were run longer if the potential scale reduction factor (*prsf*) was initially superior to 1.10. Finally, all models had potential scale reduction factor inferior or equal to 1.10 for all parameters, except for up to 2 Nb_y parameters in 10 models for Inarijoki, having larger *psrf* (inferior to 1.30).

Data and code availability:

The datasets used during the current study will be uploaded to a public data repository upon acceptance.

Code availability:

The custom codes used during the current study are available from the corresponding author on reasonable request.

References

1. Losos, J. B. Ecological character displacement and the study of adaptation. *Proceedings of the National Academy of Sciences of the United States of America* **97,** 5693–5695 (2000).

2. Andrew, R. L. *et al.* A road map for molecular ecology. *Molecular Ecology* **22,** 2605–2626 (2013).

3. Sharpe, D. M. T. & Hendry, A. P. Life history change in commercially exploited fish stocks: An analysis of trends across studies. *Evolutionary Applications* **2,** 260–275 (2009).

4. Teplitsky, C. & Millien, V. Climate warming and Bergmann's rule through time: Is there any evidence? *Evolutionary Applications* **7,** 156–168 (2014).

5. Gienapp, P., Teplitsky, C., Alho, J. S., Mills, J. A. & Merilä, J. Climate change and evolution: Disentangling environmental and genetic responses. *Molecular Ecology* **17,** 167–178 (2008).

6. Merilä, J. & Hendry, A. P. Climate change, adaptation, and phenotypic plasticity: The problem and the evidence. *Evolutionary Applications* **7,** 1–14 (2014).

7. Merilä, J. & Hoffmann, A. A. Evolutionary Impacts of Climate Change. *Oxford Research Encyclopedia of Environmental Science* **1,** 1–17 (2016).

8. Savolainen, O., Lascoux, M. & Merilä, J. Ecological genomics of local adaptation. *Nature Publishing Group* **14,** 807–820 (2013).

9. Crnokrak, P. & Roff, D. A. Dominance variance: Associations with selection and fitness. *Heredity* **75,** 530–540 (1995).

10. Barson, N. J. *et al.* Sex-dependent dominance at a single locus maintains variation in age at maturity in salmon. *Nature* **528,** 405–408 (2015).

11. Liang, Y. *et al.* A gene network regulated by the transcription factor VGLL3 as a promoter of sex-biased autoimmune diseases. *Nature Immunology* **18,** 152–160 (2017).

12. Fleming, I. A. Reproductive strategies of Atlantic salmon: ecology and evolution. *Fisheries, Reviews in Fish Biology and Fisheries* **6,** 349–416 (1996).

13. Mank, J. E. Population genetics of sexual conflict in the genomic era. *Nature Reviews Genetics* **18,** 721–730 (2017).

14. Chaput, G. Overview of the status of Atlantic salmon (Salmo salar) in the North Atlantic and trends in marine mortality. *ICES Journal of Marine Science* **69,** 1538–1548 (2012).

15. Erkinaro, J. *et al.* Life history variation across four decades in a diverse population complex of Atlantic salmon in a large subarctic river. *Canadian Journal of Fisheries and Aquatic Sciences* In press (2018). doi:10.1139/cjfas-2017-0343

16. Otero, J. *et al.* Contemporary ocean warming and freshwater conditions are related to later sea age at maturity in Atlantic salmon spawning in Norwegian rivers. *Ecology*

and Evolution **2,** 2192–2203 (2012).

17. Crozier, L. G. & Hutchings, J. A. Plastic and evolutionary responses to climate change in fish. *Evolutionary Applications* **7,** 68–87 (2014).

18. Vähä, J.-P., Erkinaro, J., Niemelä, E. & Primmer, C. R. Temporally stable genetic structure and low migration in an Atlantic salmon population complex: implications for conservation and management. *Evolutionary Applications* **1,** 137–154 (2008).

19. Heinimaa, S. & Heinimaa, P. Effect of the female size on egg quality and fecundity of the wild Atlantic salmon in the sub-arctic River Teno. *Boreal Environment Research* **9,** 55–62 (2004).

20. Jonsson, B., Jonsson, N. & Albretsen, J. Environmental change influences the life history of salmon Salmo salar in the North Atlantic Ocean. *Journal of Fish Biology* **88,** 618–637 (2016).

21. Ohlberger, J., Ward, E. J., Schindler, D. E. & Lewis, B. Demographic changes in Chinook salmon across the Northeast Pacific Ocean. *Fish and Fisheries* **00,** 1–14 (2018).

22. Friedland, K. D. *et al.* The recruitment of Atlantic salmon in Europe. *ICES Journal of Marine Science* **66,** 289–304 (2009).

23. Frainer, A. *et al.* Climate-driven changes in functional biogeography of Arctic marine fish communities. *Proceedings of the National Academy of Sciences* **114,** 12202–12207 (2017).

24. Kortsch, S. *et al.* Climate change alters the structure of arctic marine food webs due to poleward shifts of boreal generalists. *Proceedings of the Royal Society B* **282,** 20151546 (2015).

25. Jensen, A. J. Cessation of the Norwegian drift net fishery: changes observed in Norwegian and Russian populations of Atlantic salmon. *ICES Journal of Marine Science* **56,** 84–95 (1999).

26. Kuparinen, A. & Hutchings, J. A. Genetic architecture of age at maturity can generate either directional or divergent and disruptive harvest-induced evolution. *Philosophical Transactions of the Royal Society B: Biological Sciences* **372,** 20160035 (2016).

27. Hjermann, D. Ø., Ottersen, G. & Stenseth, N. C. Competition among fishermen and fish causes the collapse of Barents Sea capelin. *Proceedings of the National Academy of Sciences of the United States of America* **101,** 11679–11684 (2004).

28. Ghalambor, C. K., McKay, J. K., Carroll, S. P. & Reznick, D. N. Adaptive versus non-adaptive phenotypic plasticity and the potential for contemporary adaptation in new environments. *Functional Ecology* **21,** 394–407 (2007).

29. Schindler, D. E. *et al.* Population diversity and the portfolio effect in an exploited species. *Nature* **465,** 609–12 (2010).

30. Vähä, J.-P., Erkinaro, J., Niemelä, E. & Primmer, C. R. Life-history and habitat features influence the within-river genetic structure of Atlantic salmon. *Molecular ecology* **16,** 2638–54 (2007).

573 31. Vähä, J., Erkinaro, J., Falkegård, M., Orell, P. & Niemelä, E. Genetic stock
574 identification of Atlantic salmon and its evaluation in a large population complex.
575 *Canadian Journal of Fisheries and Aquatic Sciences* **12,** 1–12 (2016).

576 32. ICES. Report of the Baltic salmon and trout assessment working group (WGBAST).
577 3–12 (2013).

578 33. Pritchard, V. L. *et al.* Genomic signatures of fine-scale local selection in atlantic
579 salmon suggest involvement of sexual maturation, energy homeostasis, and immune
580 defence-related genes. *Molecular Ecology* In press (2018). doi:10.1111/mec.14705

581 34. ICES. Report of the Workshop on Age Determination of Salmon (WKADS). ICES
582 Document CM 2011/ACOM:44 66pp. 18–20 (2011).

583 35. Niemelä, E. *et al.* Temporal variation in abundance, return rate and life histories of
584 previously spawned Atlantic salmon in a large subarctic river. *Journal of Fish Biology*
585 **68,** 1222–1240 (2006).

586 36. Niemelä, E. *et al.* Previously spawned Atlantic salmon ascend a large subarctic river
587 earlier than their maiden counterparts. *Journal of Fish Biology* **69,** 1151–1163 (2006).

588 37. Aykanat, T., Pritchard, V. L., Lindqvist, M. & Primmer, C. R. From population
589 genomics to conservation and management: a workflow for targeted analysis of
590 markers identified using genome-wide approaches in Atlantic salmon. *Journal of Fish*
591 *Biology* **89,** 2658–2679 (2016).

592 38. Falush, D., Stephens, M. & Pritchard, J. K. Inference of population structure using
593 multilocus genotype data: Linked loci and correlated allele frequencies. *Genetics* **164,**
594 1567–1587 (2003).

595 39. Evanno, G., Regnaut, S. & Goudet, J. Detecting the number of clusters of individuals
596 using the software STRUCTURE: A simulation study. *Molecular Ecology* **14,** 2611–
597 2620 (2005).

598 40. Earl, D. A. & vonHoldt, B. M. STRUCTURE HARVESTER: A website and program
599 for visualizing STRUCTURE output and implementing the Evanno method.
600 *Conservation Genetics Resources* **4,** 359–361 (2012).

601 41. Goudet, J., Raymond, M., De Meeüs, T. & Rousset, F. Testing differentiation in
602 diploid populations. *Genetics* **144,** 1933–1940 (1996).

603 42. Wood, S. N. Fast stable restricted maximum likelihood and marginal likelihood
604 estimation of semiparametric generalized linear models. *Journal of the Royal*
605 *Statistical Society. Series B: Statistical Methodology* **73,** 3–36 (2011).

606 43. R Core Team. R: The R Project for Statistical Computing. (2017).

607 44. Venables, W. N. & Ripley, B. D. *Modern Applied Statistics With S*. (Springer, 2002).

608 45. Fox, J. Effect Displays in R for Generalised Linear Models. *Journal of statistical*
609 *software* **8,** 1–27 (2003).

610 46. Tataru, P., Simonsen, M., Bataillon, T. & Hobolth, A. Statistical Inference in the
611 Wright–Fisher Model Using Allele Frequency Data. *Systematic Biology* **66,** e30–e46

(2017).

47. Wright, S. Evolution in mendelian populations. *Genetics* **16,** 97–159 (1931).

48. Fisher, R. A. *The Genetical Theory Of Natural Selection*. (Oxford: Clarendon, 1930).

49. Brooks, S. P. B. & Gelman, A. G. General methods for monitoring convergence of iterative simulations. *Journal of computational and graphical statistics* **7,** 434–455 (1998).

50. Lenth, R. V. Least-Squares Means: The *R* Package **lsmeans**. *Journal of Statistical Software* **69,** (2016).

51. Gompert, Z. Bayesian inference of selection in a heterogeneous environment from genetic time-series data. *Molecular Ecology* **25,** 121–134 (2016).

52. Foll, M., Shim, H. & Jensen, J. D. WFABC: A Wright-Fisher ABC-based approach for inferring effective population sizes and selection coefficients from time-sampled data. *Molecular Ecology Resources* **15,** 87–98 (2015).

53. Waples, R. S. A bias correction for estimates of effective population size based on linkage disequilibrium at unlinked gene loci. *Conservation Genetics* **7,** 167–184 (2006).

54. Do, C. *et al.* NeEstimator v2: Re-implementation of software for the estimation of contemporary effective population size (Ne) from genetic data. *Molecular Ecology Resources* **14,** 209–214 (2014).

55. Waples, R. S. & Yokota, M. Temporal estimates of effective population size in species with overlapping generations. *Genetics* **175,** 219–233 (2007).

56. Belgorodski, N., Greiner, M., Tolksdorf, K. & Schueller, K. rriskDistributions: Fitting Distributions to Given Data or Known Quantiles. R package version 2.0. *R Found. Stat. Comput., Vienna.* (2017).

57. Allendorf, F. W. & Luikart, G. *Conservation and the genetics of populations*. (Blackwell Pub, 2007).

58. Plummer, M. JAGS Version 4.3.0 user manual. (2017).

59. Burnham, K. P., Anderson, D. R. & Burnham, K. P. *Model selection and multimodel inference : a practical information-theoretic approach*. (Springer, 2002).

60. Kinnison, M. T. & Hendry, A. P. The pace of modern life. II. From rates to pattern and process. *Genetica* **112–113,** 145–164 (2001).

Acknowledgements

We thank numerous fishers who participated in the collection of scales and phenotypic information, Eero Niemelä for starting the program and looking after contacts with fishers over the 40 year study period, Jorma Kuusela for organizing the samples collection from the archive and several scale readers, especially Jari Haantie. This project received funding from the European Research Council (ERC) under the European Union's Horizon 2020 research and innovation programme (grant agreement No 742312) as well as from the Academy of Finland (projects No. 284941, 286334, 307593, 302873 and 318939)

Author contributions

J.E and P.O. coordinated the collection of samples; C.R.P., Y.C., T.A. and J.E. designed the study; Y.C. analyzed the data; Y.C., C.P. and T.A. wrote the manuscript and all authors contributed to its revision.

Competing interests

The authors declare no competing financial interests.

Correspondence and requests for materials should be addressed to C.R.P.